JOURNAL OF GEOPHYSICAL RESEARCH, VOL. 100, NO. D10, PAGES 20,913–20,926, OCTOBER 20, 1995

O_3, NO_y, and NO_x/NO_y in the upper troposphere of the equatorial Pacific

I. A. Folkins[1], A. J. Weinheimer[2], B. A. Ridley[2], J. G. Walega[2], B. Anderson[3], J. E. Collins[6], G. Sachse[3], R. F. Pueschel[4] and D. R. Blake[5]

Abstract. Two of the DC-8 flights during the 1991-1992 second Airborne Arctic Stratospheric Expedition (AASE 2) were between California and Tahiti. Extremely abrupt changes in O_3 and NO_y were observed on both flights as the aircraft crossed the subtropical jet. They indicate that the width of the transition from midlatitude to tropical air in the troposphere can be as short as 1 km. The NO_y/O_3 ratio was remarkably stable across the transition. We discuss some of the dynamical features associated with the transitions and speculate on the reasons for their abruptness. They occurred south of the subtropical frontal zone and were accompanied by changes in humidity, NO_x/NO_y, and modest changes in CO, CH_4, and CO_2. In addition, a chemical model constrained by measurements of the long-lived species is used to simulate the variation of NO_x/NO_y along the two flight tracks. Although this model is quite successful at simulating observed NO_x/NO_y in midlatitude air, it drastically overestimates NO_x/NO_y in tropical air. The rate at which the model converts NO_x to HNO_3 via the NO_2 + OH reaction is very slow in the upper tropical troposphere because the low O_3 concentrations and cold temperatures force most of the NO_x to be in the form of NO during the day. We argue that there is an important NO to NO_2 pathway in this region not presently included in models, that much of the NO_y is in a stable (possibly aerosol) form that is not readily converted to NO_x, or that there has been insufficient time since convection for NO_x to be released from other more stable forms of NO_y. It is important to resolve this discrepancy because present models which have the correct O_3 and NO_y may overestimate O_3 production rates and OH concentrations in the upper tropical troposphere.

Introduction

Although the tropics contain almost one half of the Earth's atmosphere, the distribution of long-lived and radical species in the upper tropical troposphere is not well characterized. This paper examines measurements of O_3, NO_x (= NO + NO_2), NO_y (= NO + NO_2 + HNO_3 + PAN + organic nitrates + NO_3^- + ...), CO, CH_4, and CO_2 taken during flights between California and Tahiti at an altitude of 10-12 km during the winter of 1992. The first part of the paper focuses on extremely abrupt changes in O_3 and NO_y observed near the subtropical jet. It is important to characterize the transition between midlatitude and tropical air in a dynamical sense because it gives an indication of the "strength" of the Intertropical Convergence Zone (ITCZ). That is, to what extent is convection along the ITCZ able to reduce tropospheric O_3 on a global scale by pumping low O_3 marine boundary layer (MBL) air into the upper troposphere? The measurements also give some indication of the degree of mixing between tropical and midlatitude air in the upper troposphere. This helps address the question of whether the tropics are likely to remain in their relatively pristine present state despite increases in midlatitude northern hemispheric O_3 and NO_y. A midlatitude air parcel entering the tropics after being entrained into the Marine Boundary Layer (MBL) can be expected to have its O_3 and NO_y content progressively reduced by photochemical loss, deposition to the sea surface, and rainout as it approaches the ITCZ. However, since these processes occur more slowly at higher altitudes, there is more likely to be a significant interhemispheric transport of O_3 and NO_y if there is also some flow taking place in the middle and upper troposphere.

The second part of the paper deals mainly with the observed NO_x/NO_y ratios. These are interpreted with the help of a zero-dimensional photo-

[1]Atmospheric Science Program, Departments of Oceanography and Physics, Dalhousie University, Halifax, Nova Scotia, Canada.
[2]Atmospheric Chemistry Division, National Center for Atmospheric Research, Boulder, Colorado.
[3]NASA Langley Research Center, Hampton, Virginia.
[4]NASA Ames Research Center, Moffett Field, California.
[5]Department of Chemistry, University of California, Irvine, California.
[6]Science and Technology Corporation, Hampton Virginia.

Paper number 95JD01637.
0148-0227/95/95JD01637$05.00

chemical model constrained by the long-lived species measurements. This model substantially overpredicts NO_x/NO_y throughout the tropics. Although there are uncertainties associated with the presence of unmeasured NO_x reservoirs whose existence is not taken into account by the model, especially nitrate on particles NO_3^-, the magnitude of the discrepancy suggests that there is a chemical process affecting the balance between NO_x and HNO_3 not now included in models.

Meteorological Context and Chemical Tracers

The DC-8 left Moffett Field at 0700 UT on January 28, 1992, and landed in Tahiti 10 hours later. It left Tahiti at 2200 UT on January 29 and arrived at Moffett Field at 0800 UT on January 30. Apart from a brief segment during the return flight, the flights occurred entirely in the upper troposphere at an altitude of about 12 km. The tracks of these two flights are superimposed on Geostationary Operational Environmental Satellite (GOES) infrared images in Figure 1.The image in Figure 1a was taken near the midpoint of the flight at 1101 UT on January 28. The image in Figure 1b was taken 2 hours into the return flight. The coldest regions appear white and indicate the presence of high cirrus cloud; the darkest shades represent emission from warm regions of the Earth's surface. A prominent feature of both images is the tropical cyclone south of Hawaii centered at 5° N. During the flight to Tahiti, high level cirrus clouds spiraling outward from the tropical storm appear to intersect the DC-8 flight path. This can be verified by inspection of the aerosol surface area measurements given in Plate 2a. Clusters of cloud near the equator stretching west from Ecuador are associated with the ITCZ.

O_3 and NO_y were measured during the flights by chemiluminescent detectors [*Ridley et al.*, 1994] and are shown in Plate 1. The most striking aspect of these measurements are the sudden decreases in O_3 and NO_y at 23.4° N during the flight to Tahiti and the increases at 12.9° N on the return flight. These changes occurred within a horizontal distance of about 1 km, and are indicated in the satellite images of Figure 1 by horizontal lines. They were not associated with any change in altitude of the DC-8, and occurred entirely within the

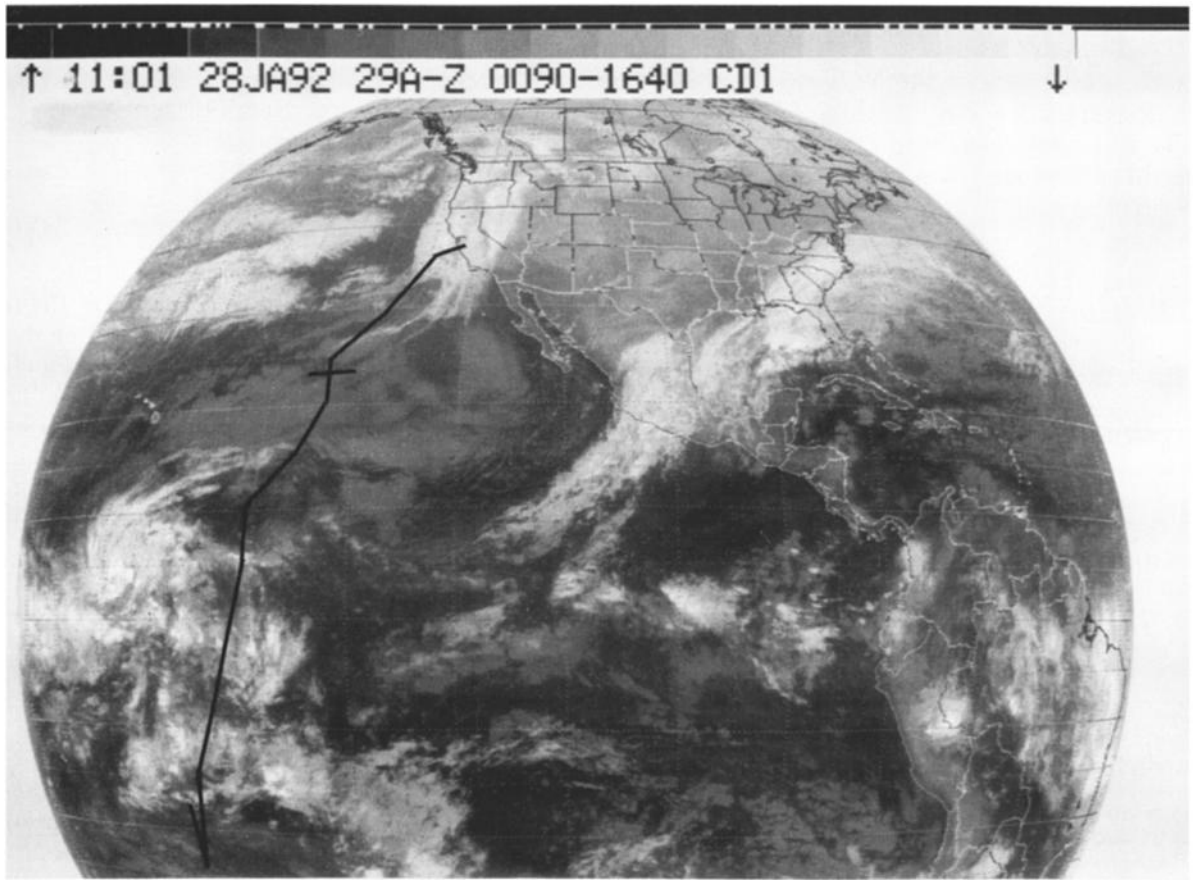

Figure 1. a. The DC-8 flight track from Moffett Field, California to Tahiti superimposed on a GOES infrared image for 1101 UT January 28, 1992. The horizontal bar corresponds to the location of the sudden O_3 and NO_y changes.
b. The DC-8 flight track from Tahiti to Moffett Field, California on January 29, superimposed on a GOES infrared image for 0001 on January 30, 1992. The horizontal bar corresponds to the location of the sudden O_3 and NO_y changes.

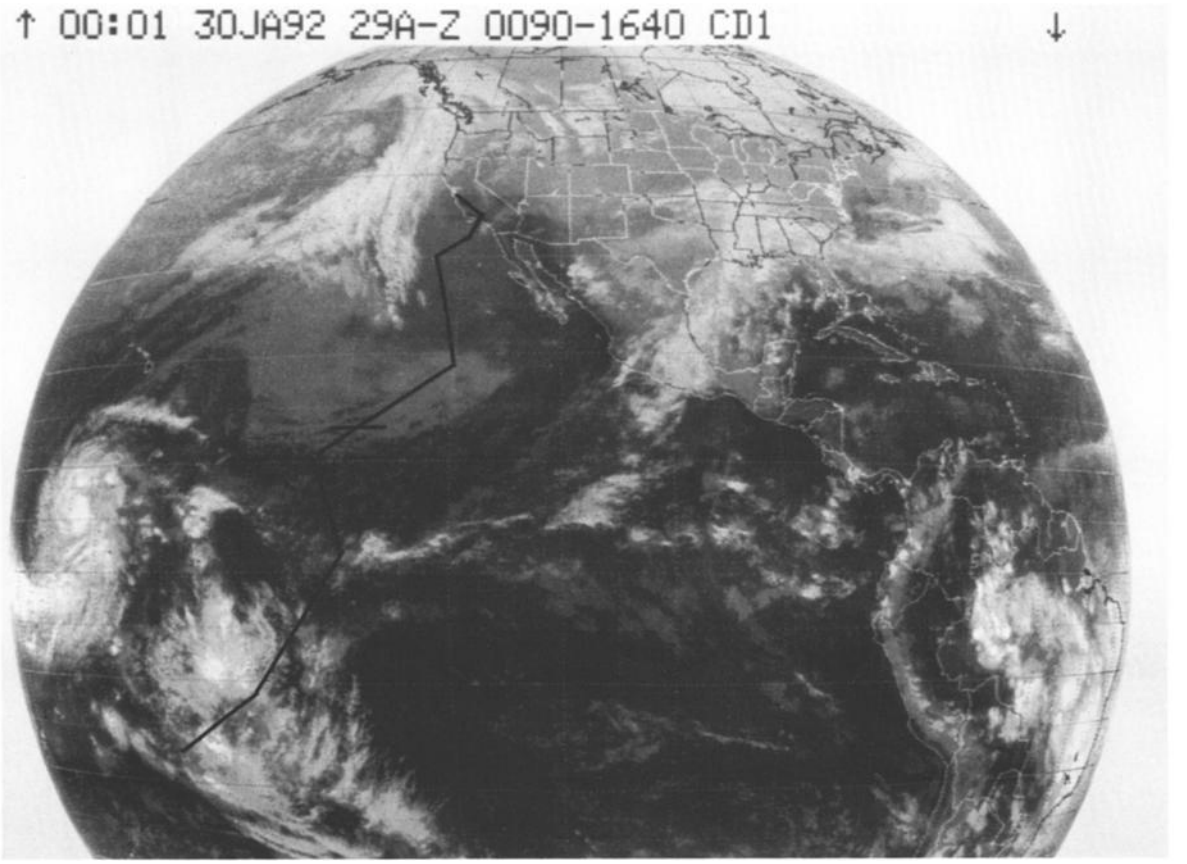

Figure 1. (continued)

troposphere. The largest values of O_3 and NO_y were associated with the stratospheric portion of the return flight between 32° and 35°.

The bias and precision errors of NO_y and O_3 depend on a variety of factors including aircraft altitude and ambient concentration. An extensive discussion of the O_3 and NO_y instruments and their associated uncertainties is given in *Ridley et al.* [1994]. For the tropical segments of the two flights, and two second integrations given in Plate 1, bias errors in NO_y are anticipated to be less than 20 parts per trillion by volume (pptv), and precision errors 26 pptv or less. The precision errors in O_3 are 2% or smaller for O_3 mixing ratios above 10 ppbv.

Plate 1 also shows NO_y/O_3. This ratio showed remarkably little change at the midlatitude to tropical transitions discussed above. As expected, the ratio is smaller and shows much less variability during the brief stratospheric segment between 32° N and 35° N than in the troposphere [*Murphy et al.*, 1993]. It has also been shown that this ratio is rather uniform in aged free tropospheric air [*Hübler et al.*, 1992a,b; *Ridley et al.*, 1994]. This was certainly true of the midlatitude portion of the January 29 flight, during which NO_y and O_3 exhibited a high degree of correlation, and the variation in NO_y/O_3 was much less than the individual variations of O_3 and NO_y. The NO_y/O_3 ratio was much less constant in the tropics, where NO_y and O_3 appear to be only weakly correlated. NO_y was rather featureless, so that the NO_y/O_3 variations arose mostly from variations in O_3, especially during the January 28 flight.

The top panel in each of Plate 1a and 1b show O_3 and NO_y probability distributions obtained from the tropical portions of the two flights. For the most part, O_3 was confined to a range of between 10 and 22 parts per billion by volume (ppbv). The NO_y distributions during the two flights were characterized by a single peak. This peak occurred at 215 pptv on the January 28 flight, and at 165 pptv on January 29.

Figure 2 shows curtain plots of temperature and wind speed along the DC-8 flight tracks.These quantities were obtained from 12 hourly European Centre for Medium Range Weather Forecasts (ECMWF) data, and linearly interpolated in space and time to locations above and below the DC-8 position. They give an indication of the vertical structure of the atmosphere during the flights. The most prominent feature in the wind speed was the subtropical jet. It was centered at 28° N during the flight to Tahiti, just above the DC-8 altitude. The jet had a multiple core during the return flight. The main branch moved south to 15° N and was considerably weaker. The location of the O_3 and NO_y changes is indicated on the figures, and on both flights, occurred on the equatorial side of the subtropical jet. Also indicated on the figures is a zone of enhanced baroclinicity extending southward and downward below the subtropical jet. This layer of air is referred to as the subtropical frontal zone and marks the dynamical boundary

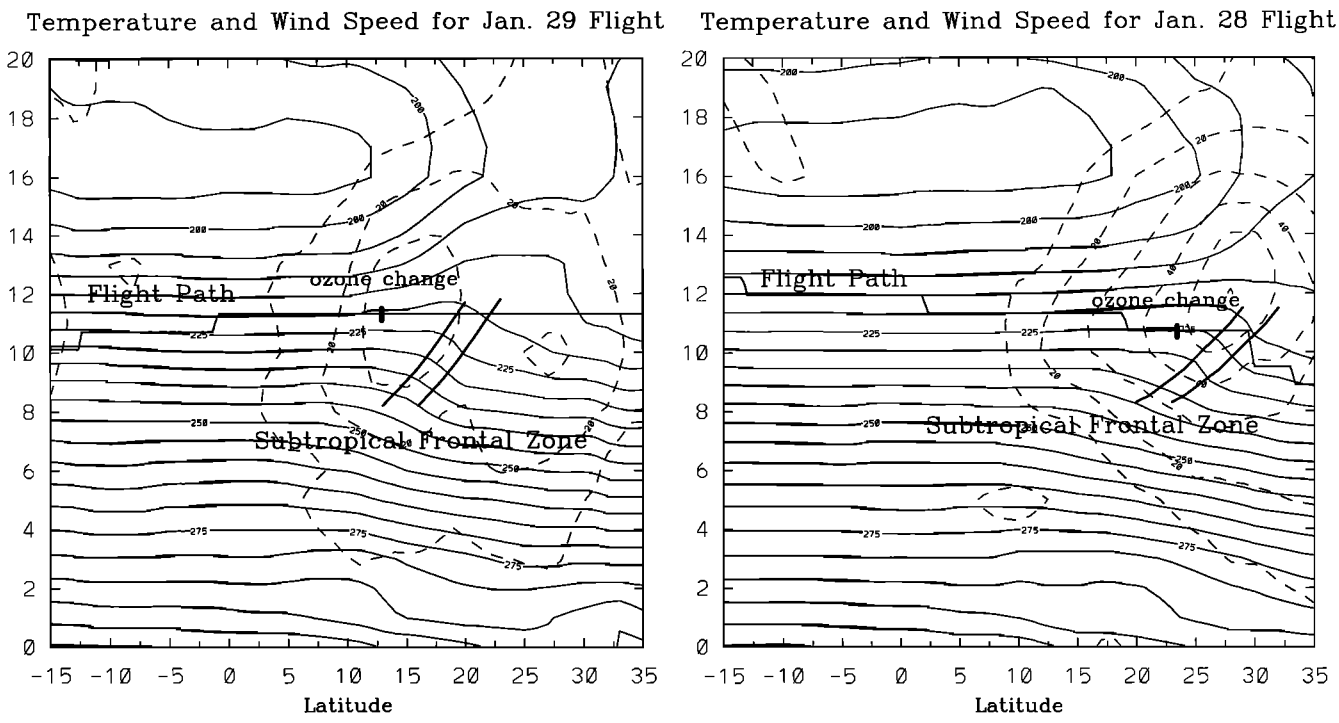

Figure 2. a. Curtain plot of ECMWF temperature and wind speed above and below the aircraft flight track during the January 28 flight. The temperature contour interval is 10 K, and the wind speed contour interval is 10 m/sec. The vertical axis is pressure height. The subtropical frontal zone is a region of enhanced baroclinicity and its approximate location is given by the slanted solid lines. The observed in situ wind speed is not shown but is consistent with the winds speeds and position of the subtropical jet given here.
b. Curtain plot of ECMWF temperature and zonal wind speed above and below the aircraft flight track during the January 29 flight.

between midlatitude and tropical air [*Palmén and Newton*, 1969]. The O_3 and NO_y changes were positioned to the south of this zone on both flights.

Three-day back trajectories from various points along the January 28 and 29 flights tracks are shown in Figures 3a and 3b. They were generated by a model [*Schoeberl et al.*, 1993a] using balanced winds on isentropic surfaces from the National Meteorological Center. The validity of the balanced winds becomes progressively dubious as the equator is approached. The trajectories should, however, be qualitatively correct outside the equatorial region. Figure 3a shows that the O_3 transition on January 28 at 23.4° N (indicated by the circle) lies between two very different back trajectories: the back trajectory intersecting the flight track at 20.0° N originating 3 days earlier over the central Pacific and the 23.8° N back trajectory originating 3 days earlier over southeast Asia. As shown in Figure 3b, the O_3 change on January 29 is slightly to the north of the most southerly of the back trajectories originating from southeast Asia, which intersects the DC-8 at 12.4° N. This is not quite consistent with the association of the O_3 change on January 28 with a change in source region: air on the high O_3 side being carried by the subtropical jet from midlatitudes, and air on the low O_3 side being recently entrained into the subtropical jet from more stagnant air in the tropical Pacific. The slight discrepancy may be attributable to one of the sources of error in the back trajectories mentioned above.

In situ measurements of local and frost point temperature [*Gaines et al.*, 1992] are shown in Plate 2. The accuracy and response time of the frost point hygrometer is poor at the cold temperatures characteristic of the two flights. The O_3 change at the 23.4° N transition from midlatitude to tropical air during the flight to Tahiti was coincident with an increase in humidity. This was also true of the return flight, although in this case the magnitude of the frost point temperature change was somewhat smaller. This is consistent with measurements of *Routhier and Davies*, [1980] taken from the mid-troposphere during flights between California and New Zealand.

The locations of the subtropical frontal zones given in the ECMWF curtain plots are consistent with the in situ temperature measurement. The temperature decrease associated with the ascent of the DC-8 from 9.5 to 10.7 km at 29.6° N during the January 28 flight occurs just north of the large arrow in Plate 2a. According to the curtain plot shown in Figure 2a, the DC-8 should have entered the subtropical frontal zone during this ascent and encountered progressively warmer temperatures as it flew south along a constant pressure surface within this zone. Plate 2a also shows a smooth increase in temperature for several degrees south of this ascent. The ECMWF and in situ subtropical frontal zone positions were also coincident during the return flight. Fig-

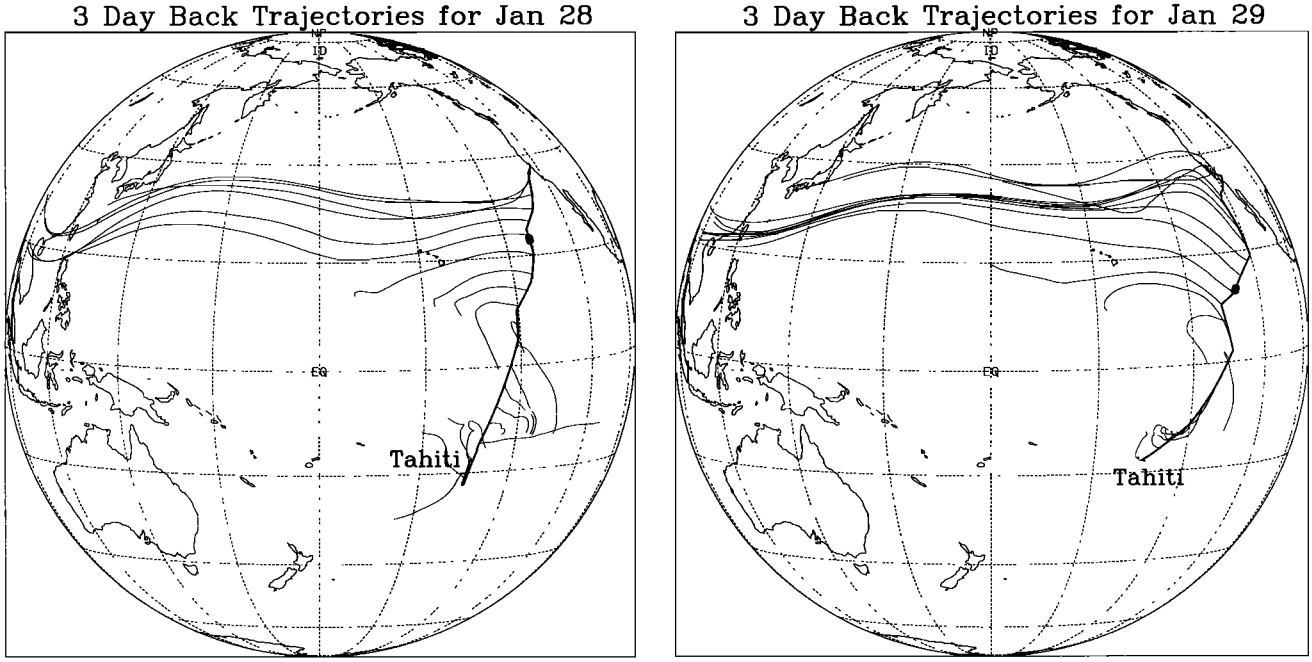

Figure 3. **a.** Three-day back trajectories from National Meteorological Center Data for the January 28 flight to Tahiti. The large dot on the flight track is the location of the sudden O_3 and NO_y changes.
b. Three-day back trajectories from National Meteorological Center Data for the January 29 flight to Moffett Field. The large dot on the flight track is the location of the sudden O_3 and NO_y changes.

ure 2b indicates that frontal zone was centered at 20° N, which is consistent with a temperature decrease of several degrees at this same latitude in Plate 2b, unassociated with any change in DC-8 pressure altitude.

The abruptness of the transitions may be attributable simply to the short period of time the two air masses are likely to have been in contact. However, there are a variety of flow configurations which can intensify horizontal gradients, some of which may have played a role in maintaining, or enhancing, the sharpness of the observed gradients. One of these is wind shear. Recently convected air parcels will be sheared as they move north away from the equator and become accelerated into the subtropical jet. This shear may have been sufficiently strong to elongate air parcels into long filaments, a process which tends to sharpen tracer gradients perpendicular to the axis of the filament [*Schoeberl et al.*, 1993b]. Three-dimensional simulations of the dispersal of the volcanic cloud from the eruption of Mt. Pinatubo show aerosol being transported from the upper tropical troposphere to the extra tropics in long narrow filaments [*Boville et al.*, 1991]. However, sharp vertical gradients of O_3 and NO_y are frequently seen in the subtropics and usually attributed to the interleaving of tropical and midlatitude air [e.g., *Hübler et al.*, 1992a]. This is referred to as "layering". If this phenomenon is related to the rapid O_3 and NO_y changes observed here, one would expect that they arose from an air mass boundary that was primarily horizontal, with a slight inclination to pressure surfaces. In the absence of information on the three-dimensional structure of the transition, it is not possible to be certain which of the above or possibly other mechanisms might be responsible for the sharpness of the transitions. Since the O_3 and NO_y changes were observed on only two flights, it is also difficult to know whether the transition is a generic feature of the subtropical jet in the eastern Pacific, or was peculiar to the meteorological conditions of the flight period.

Aerosol surface area was obtained by measuring the concentration of particles between 0.42 μm and 23.7 μm in diameter [*Gaines et al.*, 1992], and the results plotted in Plate 2. There are no obvious changes in aerosol surface area associated with the tropical to midlatitude transitions of either flight. As mentioned previously, the infrared satellite image of Figure 1a suggests that the aerosol surface area spikes seen near 15° N during the outbound flight are due to cirrus outflow from the tropical cyclone. The regions south of 7° N on the outbound flight, and south of 3° S on the return flight, were characterized by frequently elevated aerosol surface area, presumably from cirrus clouds, and persistently high humidity, suggestive of recent convective activity.

CO, CH_4, and CO_2 [*Gaines et al.*, 1992] are also shown in Plate 2. The midlatitude to tropical transition on January 28 was coincident with a small CO decrease, little change in CH_4, and a small CO_2 increase. On the return flight, CO, CH_4, and CO_2 were all higher on the tropical side of the transition. A latitudinal gradient [*Anderson et al.*, 1993] is much more evident on January 28 than January 29. There is an obvious strong

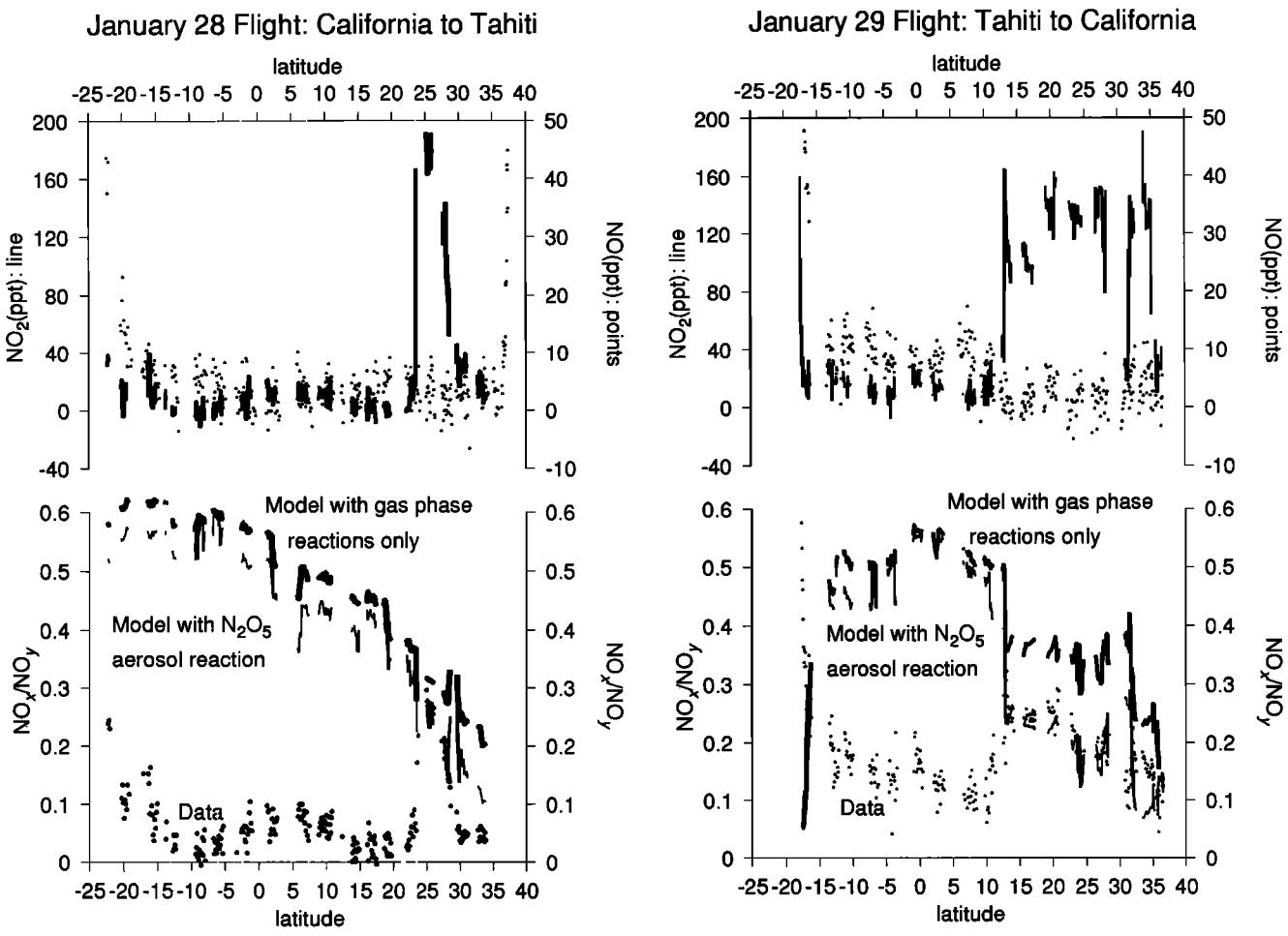

Figure 4. a. One-minute averages of NO, NO_2, and NO_x/NO_y during the January 28 flight. (bottom) This plot compares observed NO_x/NO_y with the model simulation with (thin line) and without (thick line) the N_2O_5 aerosol reaction. The thick line of the top panel refers to NO_2, while the dots refer to the measured NO. **b.** Same as for Figure 4a.

positive correlation among the three species during both the tropical and midlatitude portions of the flights. In particular, they all show a strong spike near 6° N on January 28. This peak is coincident with high aerosol surface area, ice supersaturation, and the presence of a white region in the satellite image of Figure 1a. The height and proximity of the cloud to the ITCZ suggests that this air has undergone recent deep convection from the MBL. CO, CH_4, and CO_2 are low during the stratospheric portion of the return flight between 32° N and 35° N.

Observed and Modeled NO_x/NO_y

NO and NO_2 were also measured from the DC-8 and are shown in Figure 4. The magnitudes of NO and NO_2 were frequently comparable to the calculated measurement uncertainties, particularly in the tropics where the concentrations of these compounds was extremely low. The bias and precision errors of NO during the outbound flight were 5 and 3 pptv, and for NO_2 were 16 and 8 pptv. These error estimates apply to the 1-min averages shown in Figure 4, and are valid in the limit of small NO and NO_2 (few tens of pptv or less).

The data from the January 28 flight shown in Figure 4 were taken during the night except for the segment north of 30° N. NO mixing ratios were comparable to the detection uncertainties. NO_2 mixing ratios were also usually quite low but approached 200 pptv between the ascent to dryer air at 28° N and the transition to tropical air at 23.4° N. NO_x/NO_y ratios were obtained by adding coincident values of NO and NO_2 and dividing by the average value of NO_y during the NO and NO_2 measurements. NO_x/NO_y ratios in the tropics were rarely larger than 0.1. The uncertainty in this ratio considering bias errors in NO, NO_2, and NO_y and typical tropical concentrations of these species is ± 0.07. The contribution of the stated error in NO_y to this estimate is small.

The behavior of NO and NO_2 was similar during the return flight. It occurred in daylight until 11° N, after which it remained in the dark. NO mixing ratios were typically 10 pptv during the daylight period. NO_2 mixing ratios ranged from 0 to 25 pptv in the tropics

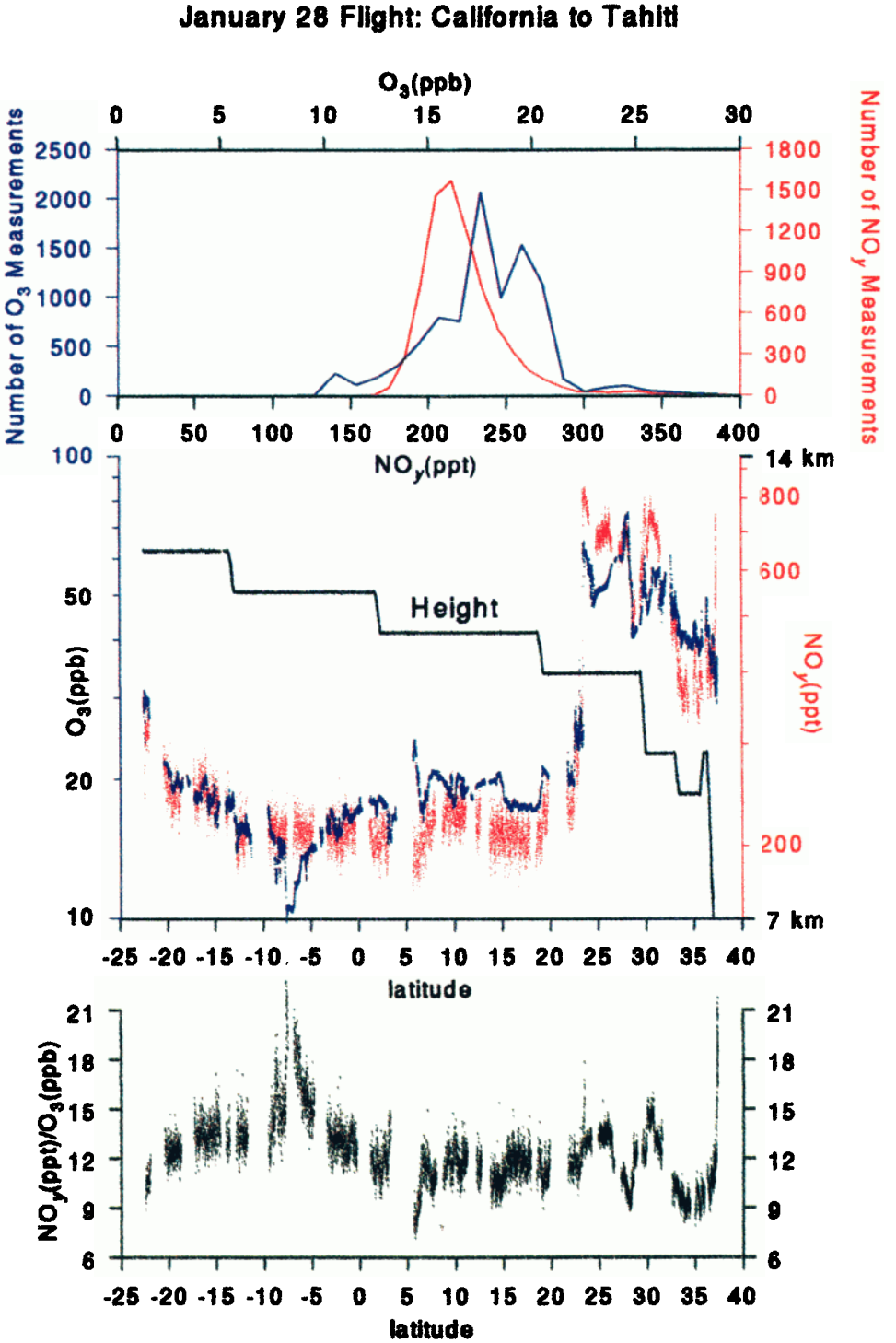

Plate 1. a. (bottom) NO_y(pptv)/O_3(ppbv) against latitude for the January 28 flight from California to Tahiti. (middle) O_3 in blue, NO_y in red, and pressure height in black. A logarithmic scale has been used for NO_y and O_3 to emphasize the tropical variability. The O_3 and NO_y measurements were made every 2 sec. (top) O_3 and NO_y probability distributions obtained from the tropical portion of the flight, defined here as the segment between the O_3 and NO_y jumps at 23.4° N and 21° N. The blue curve represents the O_3 distribution and was constructed by counting the number of O_3 measurements in each 1-ppbv interval and plotting the total versus O_3 mixing ratio.The red curve gives the NO_ydistribution and was constructed using10 pptv bins. b. O_3 and NO_y data from the January 29 return flight from Tahiti to California. Refer to the caption of Plate 1a for an explanation of each plot. The O_3 and NO_y probability distributions in the top panel were constructed from data south of the O_3 and NO_y changes at 12.9° N, and so refer to tropical air only.

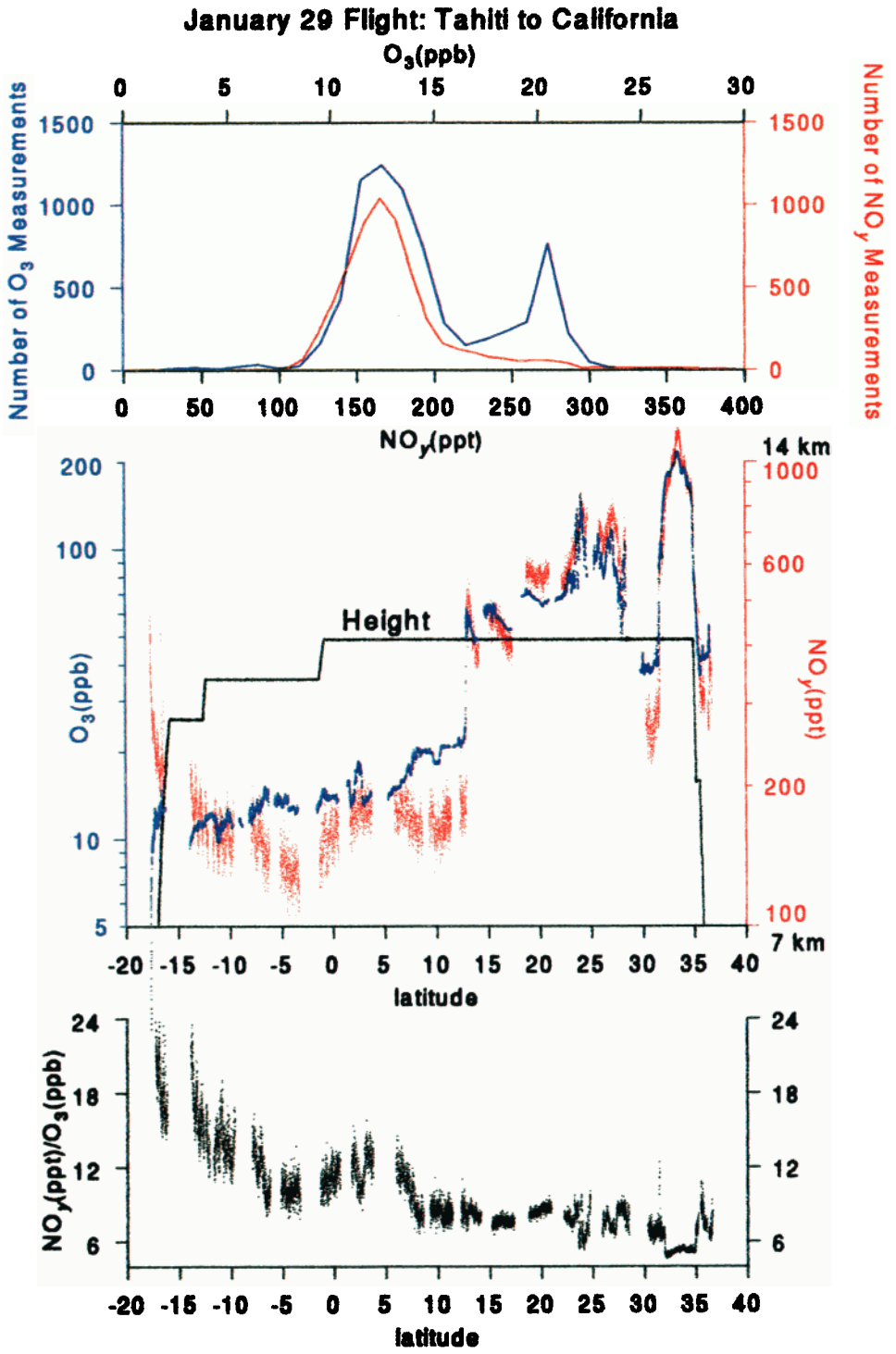

Plate 1. (continued)

but increased dramatically at the transition to midlatitude air. NO_x/NO_y ratios ranged from 0.1 to 0.2 in the tropics and also increased when the DC-8 entered midlatitude air.

Figures 4a and 4b also show modeled NO_x/NO_y ratios. These were generated by a zero-dimensional local steady state model. The model values of temperature, altitude, latitude, CH_4, NO_y, CO, C_2H_6, and O_3 were constrained to those observed during each NO_x/NO_y measurement. The H_2O mixing ratio was obtained from the frost point measurement using expressions from *Marti and Mauersberger* [1993]. The model was run for 30 days and stopped at the time of the NO_x/NO_y measurements. The resulting NO_x/NO_y ratios are plotted in Figure 4. The chemical scheme of the model is similar to that used in previous three-dimensional model simulations [*Lefèvre et al.*, 1994; *Folkins et al.*, 1994]. The chlorine and bromine species were removed be-

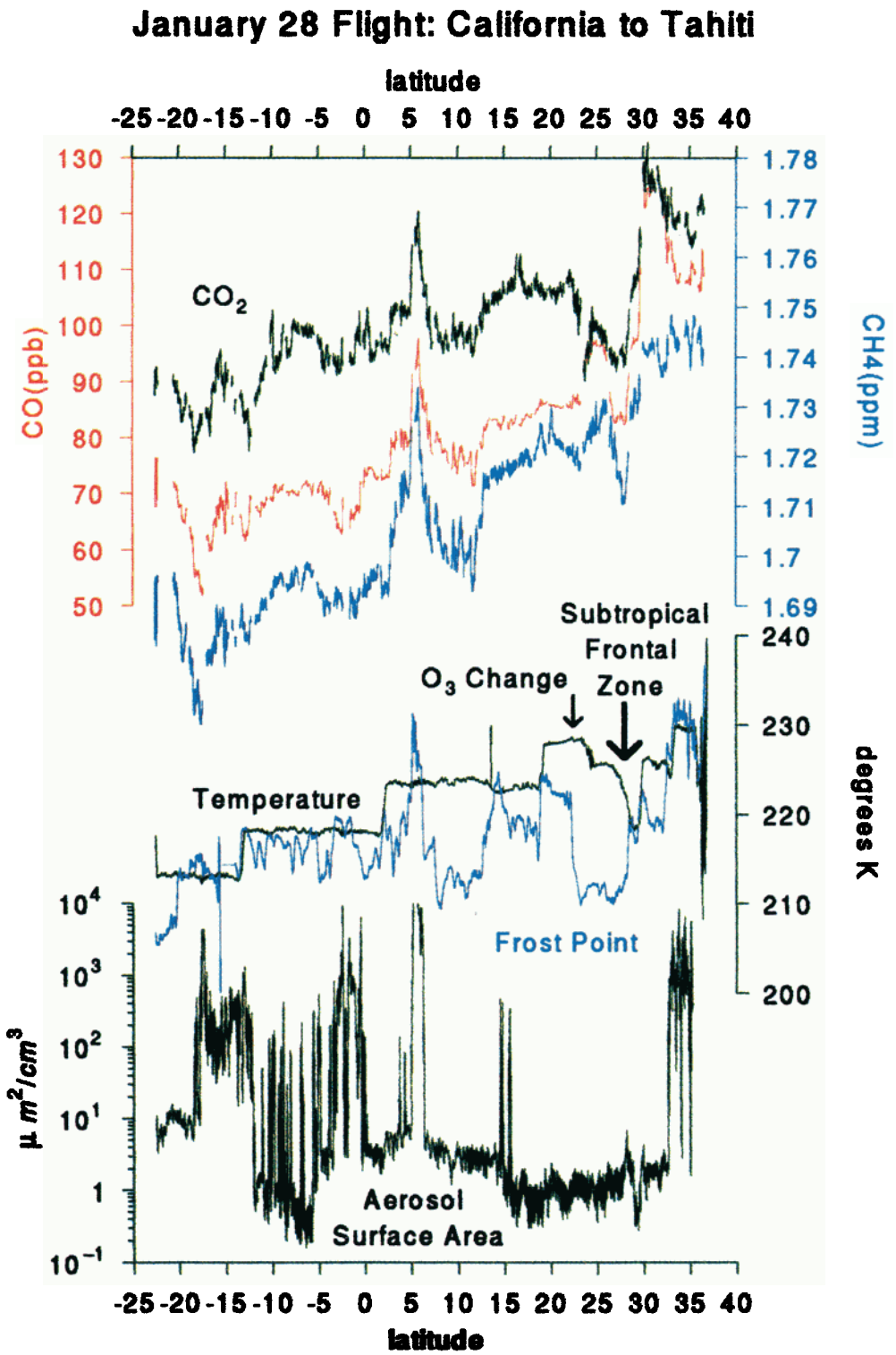

Plate 2. a. (bottom) Forward Scattering Spectrometer Probe (FSSP) aerosol surface area for the January 28 flight. Regions of elevated surface area were correlated with decreases in upwelling infrared temperature (not shown), and so are associated with proximity to clouds. (middle) Local and frost point temperature. The location of the O_3 jump shown in Plate 1a is indicated by the small arrow, and the approximate location of the subtropical frontal zone as inferred from curtain file of Figure 2a by a large arrow. The region between the O_3 change and the subtropical frontal zone was extremely dry on both flights. (top) CO_2, CO, and CH_4. The scale for CO_2 is not shown but goes from 353 ppmv at the bottom of the CH_4 scale to 357 ppmv at the top.
b. Same as Plate 2a, except that the CO_2 scale is now from 352 ppmv to 358 ppmv. The hygrometer appears to have malfunctioned between 20° and 25°, so that this data is not shown. Note that temperature is approximately constant on pressure surfaces south of the O_3 changes, so that the tropical to midlatitude O_3 increases are coincident with a transition from a barotropic to baroclinic regime.

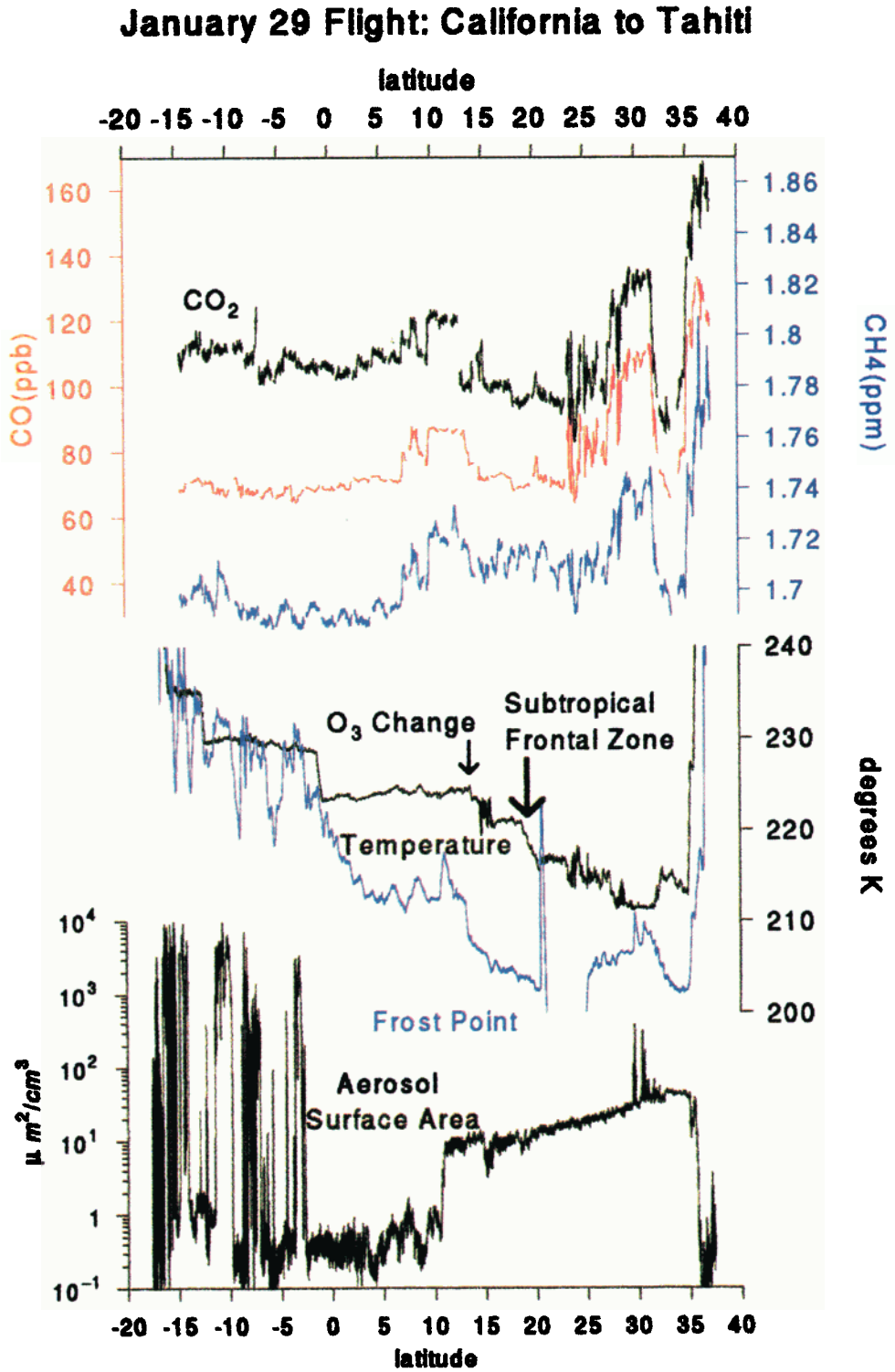

Plate 2. (continued)

cause their role in tropospheric chemistry is still largely speculative. Intermediates involved in the oxidation of C_2H_6 and formation of peroxy acetyl nitrate (PAN) have been added. A 20-day rainout loss was assigned to H_2O_2, CH_2O, CH_3OOH, CH_3OH, CH_3CHO, PAN, CH_3COOOH, and CH_3COOH. NO_y initially consisted largely of HNO_3, but the 30-day runs were sufficient to remove sensitivity of modeled NO_x/NO_y to this partitioning.

Photolysis rates were calculated every 15 min using a delta-Eddington method [*Madronich et al.*, 1987] and the latitude and altitude appropriate to each NO_x/NO_y measurement. Overhead O_3 columns were interpolated to the DC-8 flight track from Total Ozone Mapping Spectrometer (TOMS) measurements [*Gaines et al.*, 1992] and held fixed during the runs. NO_x/NO_y ra-

tios should respond to the average albedo underneath the air parcel over the past several days or weeks. This was always assumed to be 0.3. Scattering from aerosols or clouds was otherwise ignored. The absorption cross sections and quantum yields of O_3, NO_2, HO_2NO_2, N_2O_5, H_2O_2, NO_3, HONO, and CH_2O were taken from *Jet Propulsion Laboratory* (JPL) [1992], temperature-dependent HNO_3 absorption cross sections from *Burkholder et al.* [1993] and absorption cross sections of PAN from *Senum et al.* [1984].

The reaction of N_2O_5 with water on aerosol surfaces, with the release of two nitric acid molecules to the gas phase, has been demonstrated to improve modeled NO_x/NO_y ratios in the stratosphere [*Fahey et al.*, 1993; *Kawa et al.*, 1993; *Folkins et al.*, 1994]. It may play a role in lowering NO_x/NO_y in the troposphere as well [*Dentener and Crutzen*, 1993]. There is as yet no experimental evidence that this is the case. We have therefore run a simulation with gas phase reactions only, and a simulation which includes this reaction. Its first-order rate constant k is parameterized in the usual way as $k = \frac{\gamma v A}{4}$, where γ is the reaction probability, v is the mean molecular speed, and A is the aerosol surface area. The aerosol surface area A was defined using the measurements discussed above, and the reaction probability was set equal to 0.1 [*JPL*, 1992].

The local steady state model predicts an NO_x/NO_y ratio of about 0.5 in the tropics. There is a large discrepancy with the measurements in this region. The reactions which have the strongest direct effect on this ratio in the model are the reactions of OH with NO_2 and HNO_3, and HNO_3 photolysis

$$NO_2 + OH + M \rightarrow HNO_3 + M \qquad (R1)$$

$$HNO_3 + h\nu \rightarrow NO_2 + OH \qquad (R2)$$

$$HNO_3 + OH \rightarrow NO_3 + H_2O. \qquad (R3)$$

The effect of these reactions on NO_x/NO_y can be understood by examining the model output at a particular grid point. The grid point at the equator during the January 29 flight had an OH mixing ratio at noon of 0.28 pptv and a temperature of 218 K. They give rise to a lifetime for oxidation of NO_2 to HNO_3 via reaction (R1) of 13 hours. The lifetimes of nitric acid with respect to photolysis and reaction with OH at noon were 10 and 15 days. Together, they give rise to a lifetime of HNO_3 against conversion to NO_x of 6 days.

The NO_x partitioning of the model is primarily controlled by NO_2 photolysis, and the reactions of NO with O_3 and HO_2.

$$\frac{[NO]}{[NO_2]} = \frac{J_{NO_2}}{k_{NO+O_3}[O_3] + k_{NO+HO_2}[HO_2]} \qquad (1)$$

This expression evaluates to 24 using the observed 13.8 ppbv O_3 mixing ratio, a calculated 3.4 pptv HO_2 mixing ratio, and a calculated J_{NO_2} value of 0.014 sec^{-1}. The rate at which HO_2 converts NO to NO_2 is almost as fast as that of O_3. Since NO is 24 times more abundant than NO_2, the 13-hour NO_2 noon lifetime against conversion to HNO_3 represents an effective NO_x lifetime against conversion to HNO_3 of 13 days. This is approximately double the 6-day nitric acid lifetime, and would give rise to an NO_x/NO_y ratio of about 0.7. The modeled NO_x/NO_y ratio is somewhat less than this because NO_2 concentrations are largest at sunrise and sunset, so that the rate of (R1) is less strongly peaked about noon than (R2) or (R3).

To summarize, the magnitude of the modeled NO_x/NO_y ratio in the tropics is due to the degree to which NO_2 and OH are anticorrelated over a diurnal cycle. The low temperatures, strong temperature dependence of the NO + O_3 rate constant, and low O_3 concentrations make NO the dominant form of NO_x during the day and slow down the (R1) reaction rate.

The model runs do a much better job of simulating NO_x/NO_y in midlatitude air masses. This was particularly true of the model run including the N_2O_5 aerosol reaction. Its inclusion almost invariably resulted in better agreement with observed NO_x/NO_y. In most cases the degree of correspondence with this simulation is strikingly high. This suggests that our understanding of the factors regulating NO_x/NO_y in the midlatitude upper troposphere is largely correct. There are two exceptions. One occurs at the beginning of the January 28 flight at 29° N prior to an ascent to dryer air, and much higher NO_2. Parts of this section have very high aerosol surface area and are covered by clouds in the satellite photograph. The other exception occurs during the stratospheric section of the return flight between 32° N and 35° N.

The model underestimate of NO_x/NO_y during the brief stratospheric portion of the flight is consistent with previous three-dimensional modeling of the AASE 2 DC-8 flights [*Folkins et al.*, 1994]. These simulations found that although the NO_x/NO_y measurements of the March DC-8 flights strongly supported the N_2O_5 aerosol reaction, the January measurements tended to lie between the simulations with and without this reaction. It was suggested that this discrepancy may arise from the conversion of HO_2NO_2 to NO_2 within the detector. In this case, this explanation would account for about half of the difference between measured NO_x/NO_y and the NO_x/NO_y of the model run including the N_2O_5 aerosol reaction.

PAN is an important component of NO_y in many parts of the troposphere. The cold temperatures of the upper tropical troposphere inhibit its thermal decomposition and make it a stable NO_y reservoir. If present in sufficiently large concentrations, it could have significantly reduced NO_x/NO_y ratios. It is difficult to account for this in the model because PAN was not measured, and its concentrations are likely to be under dynamical rather than local photochemical control. However, measurements in tropical Pacific air masses during Chemical Instrumentation Test and Evaluation (CITE 2) indicate miniscule amounts of PAN [*Singh et al.*, 1990] and PAN to NO_x ratios less than one [*Ridley et al.*, 1990]. It is therefore unlikely that the negligible concentrations of PAN in the model account for the overestimate of tropical NO_x/NO_y ratios.

A more likely candidate for sequestering significant

amounts of NO_y in the tropics is particulate nitrate, which is known to be an important component of NO_y in the marine boundary layer. The possibility of its existence was not considered in the model. The NO_y instrument used here had an aft-facing inlet, and is expected to be sensitive to nitrate on particles less than about 0.5 μm in diameter. Particulate nitrate has been reported to be 120 pptv by mass at an altitude of 5-6 km in the northern hemisphere marine free troposphere based on 1977-1978 measurements from project Gametag [*Huebert and Lazrus*, 1980]. This corresponds to 56 pptv. Although substantial, subtracting 56 pptv from the NO_y mixing ratio used by the model would not by itself be sufficient to bring about agreement with the measured NO_x mixing ratios.

Diurnally averaged exchange times between NO_x and HNO_3 in the model are of the order of several weeks, comparable to the overturning timescale in the tropics, which is probably about a month. It is therefore likely that the assumption of local steady state by the model accounts for some of the discrepancy between observed and modeled NO_x/NO_y. Conditions at the surface favor higher daytime concentrations of NO_2 than NO, which give rise to modeled HNO_3 concentrations 3 times larger than those of NO_x [*Thompson et al.*, 1993]. The low NO_x levels of the upper tropical troposphere may therefore be attributable simply to the extremely low NO_x levels observed in marine boundary layer [*McFarland et al.*, 1979] and to the lack of time since convection for photochemical equilibrium to be established.

It is unlikely that the discrepancy arises from errors in the parameterization of the N_2O_5 aerosol reaction. There are three reactions involved in the aerosol mediated conversion of NO_x to HNO_3.

$$NO_2 + O_3 \rightarrow NO_3 + O_2 \qquad (R4)$$

$$NO_2 + NO_3 + M \rightarrow N_2O_5 + M \qquad (R5)$$

$$N_2O_5 + H_2O(\text{aerosol}) \rightarrow 2HNO_3 \qquad (R6)$$

An O_3 mixing ratio of 13.8 ppbv and a temperature of 218 K imply a lifetime for conversion of NO_2 to NO_3 via (R4) of 82 days. NO_3 photolyzes rapidly during the day, so that the formation of N_2O_5 via (R5) is possible only at night. The (R5) reaction gives rise to an NO_3 lifetime in the presence of 1 pptv of NO_2 of 29 hours. Reaction (R4) is therefore clearly the rate limiting step in the formation of N_2O_5. The low O_3 concentrations and cold temperatures make the lifetime of NO_2 with respect to (R4) very long and strongly inhibit N_2O_5 formation. This prevents the N_2O_5 aerosol reaction from having much effect on NO_x/NO_y in the tropics. This was always true in the model even though Plate 2 shows that the DC-8 flew through regions in which aerosol surface area was extremely high.

Bromoform ($CHBr_3$) has been measured in the equatorial Pacific MBL and shows a distribution strongly peaked about the equator with maximum values of 3 pptv [*Atlas et al.*, 1993]. At 220 K, 2.4 pptv of BrO converts NO to NO_2 with the same efficiency as 20 ppbv of O_3. It is quite conceivable that concentrations of BrO, in possible conjunction with ClO and IO, are sufficiently large to lower NO/NO_2 ratios in the upper equatorial troposphere. This mechanism would be particularly efficient in the presence of cirrus clouds because reactions on ice crystals, analogous to those occurring on polar stratospheric clouds, can be expected to help convert the bromine and chlorine reservoir species HBr and HCl to BrO and ClO. The NO_x/NO_y ratio in the model is however somewhat buffered against decreases in NO/NO_2 because concentrations of OH will initially decrease in response to the lower NO concentrations.

Discussion

The photochemical production of O_3 in the Pacific troposphere has been discussed using NO, CO, O_3, and H_2O measurements obtained during Global Tropospheric Experiment (GTE)/CITE 1 [*Ridley et al.*, 1987; *Chameides et al.*, 1987a]. The production of O_3 arises largely from the reactions of NO with peroxy radicals. O_3 destruction occurs via the reaction of O^1D with water. Both of these processes are quite slow at the altitudes discussed here because of the dryness of the upper troposphere and low NO concentrations. It can be shown that the crossover from net O_3 destruction to net O_3 production occurs at an NO value of 3 to 10 pptv, depending largely on the humidity. This is comparable to the uncertainty in the NO detector, so that it is hard to differentiate experimentally between the two regimes. Diurnally averaged O_3 production rates will, however, rarely be larger than 0.1 ppbv/day. Since this gives rise to an O_3 doubling time which is much longer than overturning timescale in the tropics, O_3 can be expected to behave as a quasiconservative tracer in this region. Models with the correct O_3 and NO_y will however generate unrealistically large O_3 production rates because their NO concentrations will be at least an order of magnitude larger than observed.

There are several curious features in the O_3, NO_y, and NO_y/O_3 tropical data. The first concerns the range of observed O_3 mixing ratios. Plate 2 12 shows that O_3 was largely confined to between 10 and 22 ppbv in the upper troposphere of the western equatorial Pacific. Given that O_3 is a quasiconservative tracer in this region of the atmosphere, and that O_3 mixing ratios are usually below 10 ppbv in the marine boundary layer of the ITCZ [e.g., *Thompson et al.*, 1993], it is unclear why O_3 values below 10 ppbv were never observed at DC-8 cruising altitudes. A second curious feature concerns the tropical NO_y data. The dominant forms of NO_y in the marine boundary layer are believed to be water soluble [*Liu et al.*, 1983]. If so, then air recently detrained from convective clouds should be depleted in NO_y, unless its NO_y content was enhanced by lightning, in which case it should have high NO_x levels. Tropical air depleted in NO_y or enhanced in NO_x was never observed during these two flights, even though the DC-8 flew several times through air masses which appeared to have been recently convected from the surface. Finally, although it is not surprising that O_3 and NO_y changed simultaneously at the midlatitude to tropical transition, it is unclear why their ratio remained con-

stant. This observation cannot be explained until the source of NO_y to this region of the upper tropical troposphere is determined.

High levels of NO have been observed within convective clouds over the Pacific Ocean and attributed to lightning [*Ridley et al.*, 1987; *Chameides et al.*, 1987b]. In general, however, the uniformity of tropical NO_y seen during these flights seems to run counter to the expectation [*Liu et al.*, 1983; *Murphy et al.*, 1993] that lightning is an important source of NO_y to this region of the upper tropical troposphere. It is not clear how intense localized sources of NO_y such as lightning could give rise to the featureless tropical NO_y distributions shown in Plates 1a and 1b. The conclusion of *Murphy et al.* [1993] was based in part on observations of 400 pptv of NO_y in the upper tropical troposphere over northern Australia, much larger than NO_y ratios typically observed in the tropical Pacific marine boundary layer. NO_y mixing ratios in the tropical segments of these two flights were usually between 150 and 250 pptv, which is within the range of values reported for the subtropical Pacific marine boundary layer [*Hübler et al.*, 1992a] and other estimates [*Liu et al.*, 1983]. The large islands of the western tropical Pacific give rise to a higher incidence of lightning than in the eastern tropical Pacific [*Goodman and Christian*, 1993] and may account for the larger NO_y mixing ratios discussed by *Murphy et al.* [1993].

As a source of NO_x, lightning would also tend to increase NO_x/NO_y ratios. The lifetime of NO_x against conversion to HNO_3 at the equatorial grid point discussed above was about 18 days, sufficiently long for most of the NO_x generated by lightning to remain in this form before subsidence to the flight altitudes. The actual NO_x lifetime could be much longer than 18 days because the model may overestimate OH. Running the model in a configuration, which constrained NO_x to the observed mixing ratio, left HO_x mixing ratios relatively unchanged, but decreased OH concentrations by about a factor of 3, which would give rise to a threefold increase in the lifetime of NO_x.

Conclusions

A diverse suite of compounds in the upper tropical troposphere were measured in January 1992 during flights between California and Tahiti. They yield new insights into the distribution of chemical tracers in this region. Extremely sudden changes in O_3 and NO_y during the two flights indicate the existence of a "chemical front" parallel to the subtropical jet which defines the chemical boundary between midlatitude and tropical air. The subtropical frontal zone is considered to be the dynamical boundary between midlatitude and tropical air, but occurred to the north of the O_3 and NO_y changes on both flights. We have speculated that the sharpness of the transitions may be attributable to the confluence and shearing experienced by recently convected air parcels as they move north away from the equator and encounter fast moving midlatitude air within the subtropical jet. However, this does not account for the lack of any change in aerosol surface area, so that this dynamical explanation for the sharpness of the transitions is largely conjectural. O_3 and NO_y tended to be quite homogeneous during the tropical portions of the flights and within the range of values observed in the equatorial Pacific MBL. This appears to confirm the dominant influence of convection in determining the chemical composition of the equatorial Pacific upper troposphere.

The second part of the paper deals primarily with the measurements of the short-lived radical species NO and NO_2. The model run including the N_2O_5 aerosol reaction was able to reproduce the observed variation of the NO_x/NO_y ratio during the midlatitude portions of the flights. There is therefore strong experimental evidence that this reaction does play a role in reducing NO_x/NO_y ratios in the upper midlatitude troposphere as well as the stratosphere. There is, however, some residual uncertainty associated with the presence of unmeasured nitrogen reservoir species such as PAN. When present in sufficiently large concentrations, PAN can also lower NO_x/NO_y ratios by sequestering a significant fraction of NO_y in a stable reservoir. The model did not account for this possibility.

The model comparisons also show that our present understanding of the factors controlling the NO_x/NO_y ratio in tropical air masses is poor. In this region, the model predicted ratios consistently outside the range of the measurements and strongly suggested the existence of an unknown mechanism reducing NO_x/NO_y. The main reason for the high ratios of the model was that the dominant form of NO_x during the day was NO, which slowed down the conversion of NO_x to HNO_3 via the NO_2 + OH reaction. There are several plausible explanations for the discrepancy. One explanation is that the model failed to include species which might play a role in converting NO to NO_2, such as halogen radicals. The other possibility is that much of the NO_y in this region is stored in a stable NO_y reservoir other than nitric acid, such as NO_3^-. The mechanism for reducing NO_x/NO_y may play a role in diminishing the oxidizing capacity of the upper tropical troposphere by lowering OH concentrations. It would do this both by lowering O_3 production and by favoring the partitioning of HO_x into HO_2. Simultaneous measurements of NO_y and its component species, including NO_3^-, are needed to determine the reasons for the low NO_x/NO_y ratios of the upper tropical troposphere.

Acknowledgments. The measurements were supported by the NASA High Speed Research Program and (for NCAR) the Upper Atmosphere Research Program. I. F. was supported by the Atmospheric Environment Service and the Natural Sciences and Engineering Research Council of Canada. We thank Randy Kawa for providing us with the back trajectories, Glen Lesins, Bart Geerts, and Owen Hertzman for discussions, the Atmospheric Chemistry Division at NCAR for allowing I. F. the use of their facilities during a visit when much of this paper was written, John Thoma for supplying the GOES satellite images, and an anonymous referee for helpful criticisms which lead to changes in the manuscript. NCAR is supported by the National Science Foundation.

References

Anderson, B. E., J. E. Collins, G. W. Sachse, G. W. Whiting, D. R. Blake, F. S. Rowland, AASE-II observations of trace carbon species distributions in the mid to upper troposphere, *Geophys. Res. Lett., 20*, 2539-2542, 1993.

Atlas, E., W. Pollock, J. Greenberg, L. Heidt, and A. M. Thompson, Alkyl nitrates, nonmethane hydrocarbons, and halocarbon gases over the equatorial Pacific ocean during SAGA 3, *J. Geophys. Res., 98*, 16,933-16,947, 1993.

Boville, B. A., J. R. Holton, and P. W. Mote, Simulation of the Pinatubo aerosol cloud in general circulation model, *Geophys. Res. Lett., 18*, 2281-2284, 1991.

Burkholder, J. B., R. K. Talukdar, A. R. Ravishankara, and S. Solomon, Temperature dependence of the HNO_3 UV absorption cross sections, *J. Geophys. Res., 98*, 22,937-22,948, 1993.

Chameides, W. L., et al., Net ozone photochemical production over the eastern and central North Pacific as inferred from GTE/CITE 1 observations during Fall 1983, *J. Geophys. Res., 92*, 2131-2152, 1987a.

Chameides, W. L., et al., An estimate of the NO_x production rate in electrified clouds based on NO observations from the GTE/CITE 1 Fall 1983 field operation, *J. Geophys. Res., 92*, 2153-2156, 1987b.

Dentener, F. J., and P. J. Crutzen, Reaction of N_2O_5 on tropospheric aerosols: Impact on the global distributions of NO_x, O_3, and OH, *J. Geophys. Res., 98*, 7149-7163, 1993.

Fahey, D. W., et al., In situ measurements constraining the role of reactive nitrogen and sulphate aerosols in mid-latitude ozone depletion, *Nature, 363*, 509-514, 1993.

Folkins, I., et al., Three-dimensional model interpretation of NO_x measurements from the lower stratosphere, *J. Geophys. Res., 99*, 23,117-23,129, 1994.

Gaines, S., P. Hataway, S. Hipskind, (Eds.), *Airborne Arctic Stratospheric Expedition II*, CD-ROM NASA/UARP-004, NASA Ames Res. Cent., Moffett Field, Calif., 1992.

Goodman, S. J., and H. J. Christian, Global observations of lightning, in *Atlas of Satellite Observations Related to Global Change*, edited by R. J. Guerney, J. L. Foster, and C. L. Parkinson, pp. 191-219, Cambridge University Press, New York, 1993.

Hübler, G., D. W. Fahey, B. A. Ridley, G. L. Gregory, and F. C. Fehsenfeld, Airborne measurements of total reactive odd nitrogen (NO_y), *J. Geophys. Res., 97*, 9833-9850, 1992a.

Hübler, G., et al., Total reactive oxidized nitrogen (NO_y) in the remote Pacific troposphere and its correlation with O_3 and CO: Mauna Loa Observatory photochemistry experiment 1988, *J. Geophys. Res., 97*, 10,427-10,447, 1992b.

Huebert, B. J., and A. L. Lazrus, Tropospheric gas-phase and particulate nitrate measurements, *J. Geophys. Res., 85*, 7322-7328, 1980.

Jet Propulsion Laboratory (JPL), Chemical kinetics and photochemical data for use in stratospheric modeling, in Evaluation Number 10, *JPL Publ.*, 92-20, 1992.

Kawa, S. R., et al., Interpretation of NO_x/NO_y observations from AASE-II using a model of chemistry along trajectories, *Geophys. Res. Lett., 20*, 2507-2510, 1993.

Liu, S. C., M. McFarland, D. Kley, O. Zafiriou, and B. Huebert, Tropospheric NO_x and O_3 budgets in the equatorial Pacific, *J. Geophys. Res., 88*, 1360-1368, 1983.

Lefèvre, F., G. Brasseur, I. Folkins, A. K. Smith, and P. Simon, Chemistry of the 1991-92 stratospheric winter: Three-dimensional model simulations, *J. Geophys. Res., 99*, 8183-8191, 1994.

Madronich, S., Photodissociation in the atmosphere, 1, Actinic flux and the effects of ground reflections and clouds, *J. Geophys. Res., 92*, 9740-9752, 1987.

Marti, J., and K. Mauersberger, A survey and new measurements of ice vapor pressure at temperatures between 170 and 250 K, *Geophys. Res. Lett., 20*, 363-366, 1993.

McFarland, M., D. Kley, J. W. Drummond, A. L. Schmeltekopf, and R. H. Winkler, Nitric oxide measurements in the equatorial Pacific region, *Geophys. Res. Lett., 6*, 605-608, 1979.

Murphy, D. M., et al., Reactive nitrogen and its correlation with ozone in the lower stratosphere and upper troposphere, *J. Geophys. Res., 98*, 8751-8773, 1993.

Palmén, E. C., and C. W. Newton, *Atmospheric Circulation Systems*, Academic, San Diego, Calif., 1969.

Ridley, B. A., M. A. Carroll, G. L. Gregory, Measurements of nitric oxide in the boundary layer and free troposphere over the Pacific Ocean, *J. Geophys. Res., 92*, 2025-2047, 1987.

Ridley, B. A., et al., Ratios of peroxyacetyl nitrate to active nitrogen observed during aircraft flights over the eastern Pacific Oceans and the continental United States, *J. Geophys. Res., 95*, 10,179-10,192, 1990.

Ridley, B. A., J. G. Walega, J. E. Dye, and F. E. Grahek, Distribution of NO, NO_x, NO_y, and O_3 to 12 km altitude during the summer monsoon season over New Mexico, *J. Geophys. Res., 99*, 25,519-25,534, 1994.

Routhier, F., and D. D. Davis, Free tropospheric/boundary-layer airborne measurements of H_2O over the latitude range of 58° S to 70° N: Comparison with simultaneous ozone and carbon dioxide measurements, *J. Geophys. Res., 85*, 7293-7306, 1980.

Schoeberl, M. R., S. D. Doiron, L. R. Lait, P. A. Newman, and A. J. Krueger, A simulation of the Cerro Hudson SO_2 Cloud, *J. Geophys. Res., 98*, 2949-2955, 1993a.

Schoeberl, M. R., and J. T. Bacmeister, Mixing Processes in the extra tropical stratosphere, in *The Role of the Stratosphere in Global Change*, NATO ASI Ser., vol. 18., edited by M. L. Chanin, Springer-Verlag, New York, 1993b.

Senum, G. I., Y. N. Lee, and J. S. Gaffney, Ultraviolet absorption spectrum of peroxyacetyl nitrate and peroxpropionyl nitrate, *J. Phys. Chem., 88*, 1269-1270, 1984.

Singh, H. B., et al., Peroxyacetyl Nitrate measurements during CITE 2: Atmospheric distribution and precursor relationships, *J. Geophys. Res., 95*, 10,163-10,178, 1990.

Thompson, A. M., et al., Ozone observations and a model of marine boundary layer photochemistry during SAGA 3, *J. Geophys. Res., 98*, 16,955-16,968, 1993.

B. Anderson and G. Sachse, NASA Langley Research Center, Hampton, Virginia, 23681. e-mail: b.e.anderson@larc.nasa.gov

D. R. Blake, Department of Chemistry, University of California, Irvine, CA 92717.

J. E. Collins, Science and Technology Corporation, Hampton, VA 23681. e-mail: j.e.collins@larc.nasa.gov

I. A. Folkins, Atmospheric Science Program, Departments of Oceanography and Physics, Dalhousie University, Halifax, NS, Canada B3H 4J1. (e-mail: folkins@atm.dal.ca)

R. F. Pueschel, NASA-Ames Research Center, Moffett Field, CA 94035-1000. e-mail: rudolf_pueschel@qmgate.ar.nasa.gov

B. A. Ridley, J. G. Walega, and A. J. Weinheimer, Atmospheric Chemistry Division, National Center for Atmospheric Research, Boulder, CO 80307 e-mail: wein@acd.ucar.edu

(Received November 28, 1994; revised April 17, 1995; accepted April 17, 1995.)